Vinflunine, a Novel Microtubule Inhibitor, Suppresses Calmodulin Interaction with the Microtubule-Associated Protein STOP†

Alexander A. Makarov,‡ Philipp O. Tsvetkov,‡ Claude Villard,§ Didier Esquieu,§ Bertrand Pourroy,§ Jacques Fahy,|| Diane Braguer,§ Vincent Peyrot,§ and Daniel Lafitte*,§

Engelhardt Institute of Molecular Biology, Russian Academy of Sciences, Vavilov Street 32, 119991 Moscow, Russia, CRO2 INSERM U911, Aix-Marseille University, 27 boulevard Jean Moulin, 13385 Marseille Cedex 5, France, and Institut de Recherche Pierre Fabre, Centre de Recherche en Oncologie Expérimentale, 3 rue des Satellites, 31432 Toulouse Cedex 4, France

Received May 25, 2007; Revised Manuscript Received October 15, 2007

ABSTRACT: *Vinca* alkaloids vinblastine and vincristine and some of their derivatives such as vinorelbine are widely used in therapy of leukemia and several solid tumors. Their action is associated with alterations of the mitotic spindle functions that prevent the cell cycle progression and lead to mitotic block. A number of studies show that some *Vinca* alkaloids inhibit CaM−target interaction. The newest microtubule inhibitor, vinflunine (Javlor), currently in clinical trials, is remarkably more active than vinblastine against a number of tumors. Moreover, vinflunine is significantly less toxic than other *Vinca* alkaloids. The high antitumor activity of this molecule is not well understood since it binds to tubulin with an overall affinity several-fold lower than that of vinblastine or vincristine. In this study, we examined the interaction of Ca^{2+}−CaM with vinflunine, vinblastine, and stable tubule only polypeptide (STOP) by using a combination of thermodynamic and mass spectrometric approaches. We characterized the influence of *Vinca* alkaloids on Ca^{2+}−CaM−STOP complex formation. Our results revealed different binding modes to Ca^{2+}−CaM for vinflunine and vinblastine, highlighting that adding fluorine atoms on the cleavamine moiety of the *Vinca* alkaloid molecule is critical for the localization of the drug on calmodulin. We demonstrate that vinflunine is a better inhibitor for STOP binding to calmodulin than vinblastine. We suggest that vinflunine action on calmodulin can have an effect on microtubule dynamics. These data may contribute to a better understanding of the superior antitumor efficiency and lower toxicity of vinflunine.

The dynamics and stability of microtubules are tightly controlled by numerous specialized proteins. Among them the members of the stable tubule only polypeptide (STOP)[1] family prevent the microtubule disassembly in vitro after exposure to the cold, dilution, or depolymerizing drugs (*1*, *2*). Recently, Andrieux et al. demonstrated that STOP is a major factor implicated in synaptic plasticity (*3*). In fibroblasts STOP is physiologically associated with specific microtubules of the mitotic spindle and plays a role in the cell cycle progression during mitosis. The fibroblastic form of STOP (F-STOP) binds to microtubules and is responsible for the microtubule cold stability (*4*).

Calmodulin (CaM) is known to bind STOP proteins in a calcium-dependent manner and to regulate its microtubule-stabilizing function (*5*, *6*). The colocalization of calmodulin with different STOP proteins has been demonstrated in nerve terminals and in the mitotic spindle (*7*, *8*). This observation has led to the conclusion that the Ca^{2+}−CaM−STOP complex plays a physiological role in numerous cell phenomena. Recent studies have demonstrated that all members of the STOP family have a domain that contains nearly identical multiple repeats, bearing multiple CaM binding sites. These CaM binding sites overlap with two distinct sets of microtubule-stabilizing motifs (Mc motif) (*9*). Bouvier et al. have characterized the interaction between Ca^{2+}−CaM and the STOP peptide model STP23, the 23-mer peptide corresponding to the consensus Mc motif (*10*). The results suggest that STP23 binds to CaM with an affinity of 2.5×10^5 M^{-1}, similar to that of the native protein.

Microtubule-targeted drugs affect the microtubule assembly and dynamics by different molecular mechanisms and with different sensitivities (*11*). Colchicine and *Vinca* alkaloids act as microtubule depolymerizing agents both in vitro and in vivo. The *Vinca* alkaloids vinblastine (VLB) (Figure 1) and vincristine and some of their derivatives such as vinorelbine are largely used in therapy of leukemia and several solid tumors. Their action is associated with an inhibition of microtubule dynamics in the mitotic spindle

† This work was supported by a grant from the Centre National de la Recherche Scientifique (PICS France-Russie, No. 3841, Programme Proteome), by the canceropôle and region PACA, by RFBR Grant 07-04-92165, and by the Molecular and Cellular Biology Program of the Russian Academy of Sciences.

* To whom correspondence should be addressed. Phone: +33491835680. Fax: +33491835506. E-mail: daniel.lafitte@pharmacie.univ-mrs.fr.

‡ Russian Academy of Sciences.

§ Aix-Marseille University.

|| Centre de Recherche en Oncologie Expérimentale.

[1] Abbreviations: CaM, calmodulin; STOP, stable tubule only polypeptide; F-STOP, fibroblastic form of STOP; STP23, STOP 23-mer peptide (Mc motif); ITC, isothermal titration calorimetry; DSC, differential scanning calorimetry; TFP, trifluoperazine; VLB, vinblastine; VFL, vinflunine; ESI-MS, electrospray ionization mass spectrometry.

10.1021/bi701803s CCC: $37.00
Published on Web 12/04/2007

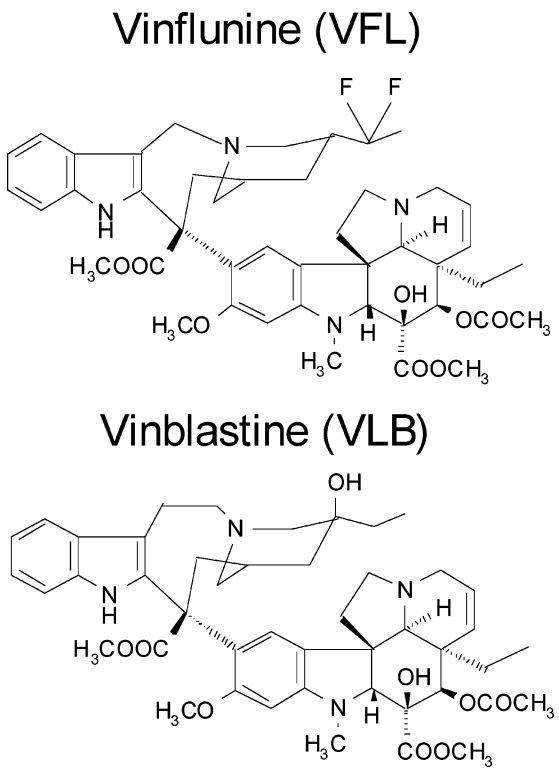

FIGURE 1: Structure of vinflunine (VFL) and vinblastine (VLB).

that lead to a mitotic block and cancer cell death (*11*−*13*). A number of studies show that some *Vinca* alkaloids inhibit CaM−target interaction (*14*). Moreover, in MDCK and HeLa cells microtubule perturbations by VLB cause the release of CaM from the pole of the mitotic spindle into a uniform cytoplasmic distribution (*15*).

The newest microtubule inhibitor, vinflunine (VFL; Javlor) (Figure 1), was created by superacid chemistry (*16*). This drug, currently in phase III clinical trials, displays a better activity than VLB against a number of murine tumors and human tumor xenografts (*17*). VFL arrests mitosis in cancer cells without significant toxic side effects (*16*). This superior antitumor activity of VFL is not well understood since it binds to tubulin with an overall affinity several-fold lower than that of VLB or vincristine (*18*). One possibility is that VFL targets not only tubulin but also other proteins, which potentiates the antitumor effect of the drug. On the basis of the work of Vertessy and co-workers (*14*), we propose that CaM could be such a target. In this study, we examined the VFL, VLB, and STP23 interaction with Ca^{2+}−CaM by a combination of thermodynamic and mass spectrometric approaches and characterized the influence of *Vinca* alkaloids on Ca^{2+}−CaM−STP23 complex formation. Results indicate the difference in binding modes to Ca^{2+}−CaM between VFL and VLB. We demonstrate that VFL is a better inhibitor for STOP binding to CaM than VLB. These data may contribute to a better understanding of the superior antitumor efficacy and lower toxicity of VFL in vivo.

EXPERIMENTAL PROCEDURES

Materials. The hybrid of mammalian and plant calmodulin, namely, SynCaM (average molecular mass 16627.3 Da), was produced and purified as described previously (*19*). The protein purity was checked by high-performance liquid chromatography and electrospray mass spectrometry coupled to an ion trap (LCQ Deca XP plus, Thermo Finnigan). The protein concentration was measured spectrophotometrically with a molar extinction coefficient of 1560 M^{-1} cm^{-1} at 280 nm (*19*). STP23, QRDTRRKAGPAWMVTRTEGHEEK, a 23-residue peptide with an average mass of 2740 Da corresponding to the calmodulin binding domain of STOP (*10*), was produced by solid-phase peptide synthesis using FMOC chemistry and purified by HPLC. The peptide concentration was determined spectrophotometrically, assuming a molar extinction coefficient of 5690 M^{-1} cm^{-1} at 280 nm. All chemicals (Sigma-Aldrich Co.) were of the highest grade. VLB (monoisotopic mass 810 Da) was from Lilly (Suresnes, France), and VFL (monoisotopic mass 816 Da) was a generous gift of Pierre Fabre (Toulouse, France).

Isothermal Titration Calorimetry (ITC). Binding of *Vinca* alkaloids, trifluoperazine (TFP), or STP23 peptide to Ca^{2+}−CaM was analyzed by ITC using either MicroCal MCS or VP-ITC instruments at 25 °C in 50 mM Hepes buffer, in the presence of 150 mM KCL and 1 mM $CaCl_2$, pH 7.5. Ca^{2+}−CaM concentrations in the calorimetric cell ranged from 0.02 to 0.03 mM, whereas the ligand (*Vinca* alkaloids, TFP, or STOP peptide) concentrations in the syringe varied from 0.7 to 2 mM. The STOP peptide binding to Ca^{2+}−CaM was carried out in the presence and in the absence of the *Vinca* alkaloids of interest. The heat of dilution was measured by injecting the ligand into the protein-free buffer solution or by additional injections of peptide after saturation; the value obtained was subtracted from the heat of reaction to obtain effective heat of binding. Data were analyzed using the MicroCal Origin software and were fitted with a model assuming one set of sites in the case of *Vinca* alkaloids or STP23 binding to CaM or a competitive binding model when one drug displaces another. The model assuming two sets of sites was the best choice for TFP binding to CaM. The affinity constant (K_a), enthalpy changes (ΔH), and stoichiometry (N) were obtained. Consequently, the Gibbs energy (ΔG) and the entropy variations (ΔS) were calculated according to the standard equations. The change in heat capacity of binding (ΔC_p) was obtained by measuring the change of the binding enthalpy over a range of temperatures from 5 to 60 °C from the relationship $\Delta C_p = d(\Delta H)/dT$, assuming that ΔH approximates to a linear function of temperature.

Differential Scanning Calorimetry (DSC). Heat denaturation measurements were carried out on a MicroCal VP-DSC instrument in 0.51 mL cells at a heating rate of 1 K min^{-1}. Experiments were performed in 50 mM Hepes buffer in the presence of 150 mM KCl and 2 mM $CaCl_2$, pH 7.5. The protein concentration varied from 1.5 to 2.1 mg mL^{-1}. Curves were corrected for the instrumental baseline obtained by heating the solvent used for the protein solution. The reversibility of denaturation was checked routinely by sample reheating after cooling in the calorimetric cell. The denaturation parameters were determined assuming that the molecular mass of CaM is 16627.3 Da and the partial specific volume is 0.72 cm^3 g^{-1} (*20*). To analyze functions of excess heat capacity, MicroCal Origin software was used. The errors in the parameters of individual transitions obtained by deconvolution of complex endotherms did not exceed ±10% for the transition enthalpy and ±0.6 °C for the transition temperature.

Electrospray Mass Spectrometry. Mass spectrometric measurements were performed on an LCQ Deca XP ion trap mass spectrometer (Thermo Finnigan) equipped with an electrospray ionization source. Samples were infused at a flow rate of 0.5 μL/min. The spray voltage was 4 kV, and the nitrogen sheath gas was set to 20 au. Full scans of *m*/*z* 1500−4000 were automatically acquired using the Excalibur 1.3 data system (Thermo Finnigan). Experiments were made in 10 mM ammonium bicarbonate buffer. CaM was used at a concentration of 15 μM.

RESULTS

Vinflunine and Vinblastine Binding to CaM. Electrospray ionization mass spectrometry (ESI-MS) is a powerful tool to monitor noncovalent interactions. It can be used under precise conditions to determine the stoichiometry of complexes (*21*). Thus, the interaction between CaM and *Vinca* alkaloids was measured by ESI-MS in 10 mM ammonium bicarbonate, a volatile buffer compatible with mass spectrometry. In the presence of a 5-fold excess of *Vinca* alkaloids (75 μM) and in the absence of calcium, the 6+, 7+, 8+, and 9+ charge states of apo-CaM and 9+, 10+, 11+, and 12+ charge states of apo-CaM dimer (CaM_2) were observed in the ESI spectrum, and no complex between CaM and *Vinca* alkaloids was detected (data not shown). In the presence of a saturating $CaCl_2$ concentration (200 μM), whether we used VLB or VFL (Figure 2), abundant 6+ and faint 5+ ions of the calcified CaM−drug complexes bearing one, two, or three *Vinca* alkaloids were detected. We also detected the charge states of calcified CaM monomer and dimer species. Peaks were broad due to the presence of calcium and sodium adducts to the protein. The predominant stoichiometry was two *Vinca* alkaloid molecules for one CaM molecule in all tested conditions. A complex with three *Vinca* alkaloid molecules was always barely detectable. Experiments were also performed with an equimolar mixture of both *Vinca* alkaloids, and the spectrum was almost the same as the spectrum with only one *Vinca* alkaloid in terms of complex intensity. The two *Vinca* alkaloids have very close masses (810 Da for VLB and 816 Da for VFL). If we consider the 6+ charge state of the calcified CaM−VFL and CaM−VLB complexes, the difference between the peaks is only 1 Da. Therefore, we could not detect by ESI-MS whether VFL or VBL alone or a mixture of both drugs was bound to CaM.

Isothermal titration calorimetry was used to monitor VFL and VLB binding to Ca^{2+}−CaM. ITC data are shown in Figure 3. The higher panel of each subset presents the raw calorimetric data for the ligand-into-protein titration, and the lower panel presents the binding isotherm. In the absence of Ca^{2+} neither of the *Vinca* alkaloids was able to bind to the protein (not shown). Direct ITC measurement showed that both drugs form a 1:1 complex with Ca^{2+}−CaM (Table 1). It was surprising to see that the binding enthalpies and entropies were drastically different: while the binding of the VLB molecule was entropy-driven, the binding of VFL was enthalpy-driven (Table 1). Calorimetry measures the totality of heat effect, generated by complex formation, protein conformational change, and also buffer ionization due to proton release upon complex formation. Experiments were performed in two buffers with different heats of ionization (47.2 kJ mol^{-1} for Tris and 20.4 kJ mol^{-1} for Hepes). The measured enthalpy of binding was independent of buffer; thus, the net flux of proton for the interaction of the two drugs with CaM was around zero. ITC experiments were also performed in the ESI-MS experimental buffer, i.e., 10 mM ammonium bicarbonate (Table 1). The thermodynamic profile of interaction was quasi identical to those recorded in Hepes or Tris.

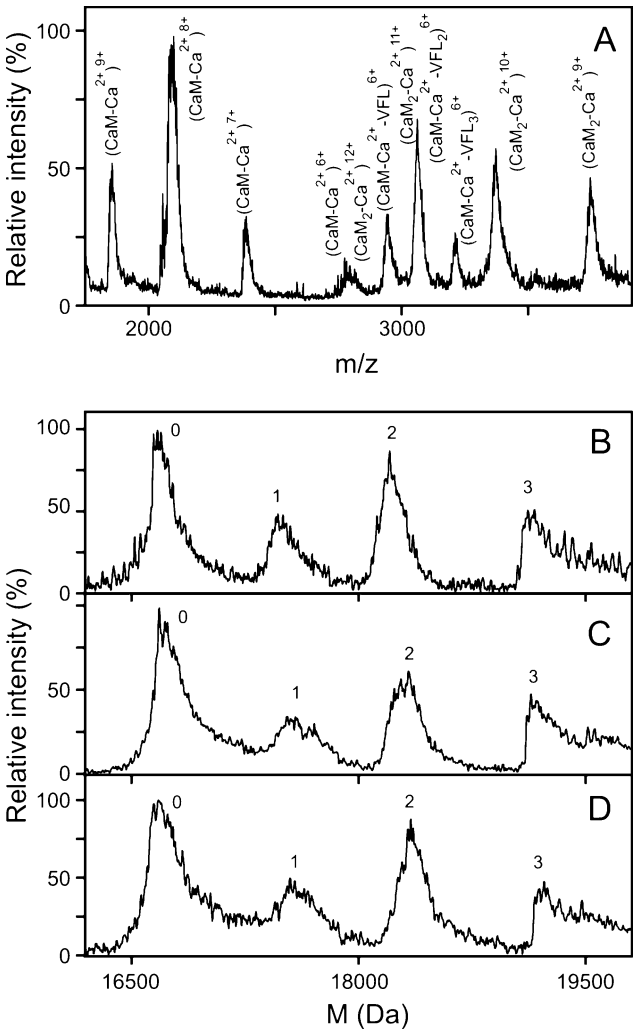

FIGURE 2: (A) ESI-MS spectrum of the Ca^{2+}−CaM−VFL complex in 10 mM ammonium bicarbonate. The concentrations were 15 μM for CaM, 75 μM for vinflunine, and 200 μM for $CaCl_2$. The most abundant species is *m*/*z* 3078.5 $(CaM-Ca^{2+}-VFL)^{6+}$, with a pronounced shoulder on *m*/*z* 3058.5 $(CaM-Ca^{2+})^{11+}$. In the labels Ca^{2+} indicates calcifed species. The most abundant species carried four calcium ions. Deconvoluted spectrum of VFL (75 μM) (B), VLB (75 μM) (C), and an equimolar mixture (75 μM VFL and 75 μM VLB) of both *Vinca* alkaloids (D) binding to CaM. In (B−D) the number of *Vinca* alkaloid molecules bound to CaM is indicated near each peak.

The change in the heat capacity of binding (ΔC_p) is an important parameter for understanding how a protein is adapted to ligand incorporation. Conformational changes can expose or hide apolar surfaces, which results in a positive (exposure) or negative (hiding) contribution to ΔC_p (*22*). In addition, ligand binding decreases the protein surface accessibility to the solvent and hides apolar surfaces that are responsible for the major positive contribution to ΔC_p (*22*). The ITC measurements were carried out between 5 and 60 °C for both *Vinca* alkaloids. The ΔH of binding was plotted against temperature (Figure 4), and the data were

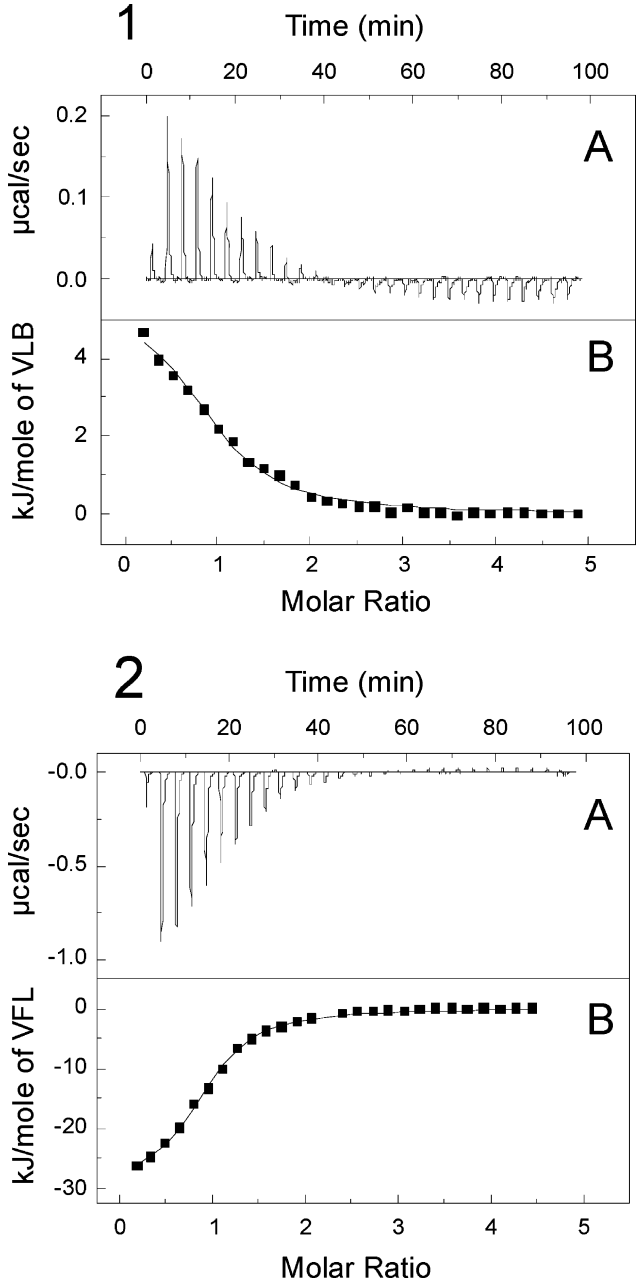

FIGURE 3: ITC curves of CaM−VLB (1) and CaM−VFL (2) interaction at 25 °C in 50 mM Hepes buffer in the presence of 2 mM $CaCl_2$, pH 7.5: (A) titration of CaM by ligand, (B) binding isotherm derived from (A).

fitted to a linear function to obtain the ΔC_p of binding. The ΔC_p values for the analyzed complexes are negative: -468 ± 12 kJ mol^{-1} K^{-1} for VFL and -361 ± 10 kJ mol^{-1} K^{-1} for VLB. Thus, ITC data demonstrate the existence of different CaM binding modes for VFL and VLB. To test whether it reflects different binding sites, we performed ITC competition experiments.

Competition between VLB and VFL for CaM Binding. VFL binding to CaM in the presence of VLB (3:1 VLB:CaM ratio, saturation conditions according to ITC titration, Figure 3) was still possible without any change in the binding constant. These data clearly show that the VFL and VLB binding sites on CaM detected by the direct ITC measurements are different. The apparent binding constant of VFL in the presence of a 15-fold excess of VLB was decreased, highlighting the competition between the two drugs for this concentration. Using the competition model, we obtained the enthalpy and binding constant for a VLB low-affinity site (Table 1). The binding constant of VLB in the presence of a 3-fold excess of VFL was not modified. In the presence of a 15-fold excess of VFL there was no ITC signal, indicating the same binding enthalpies for both *Vinca* alkaloids on this site (Table 1).

Competition between Trifluoperazine and Vinca Alkaloids for CaM Binding. It has been shown previously that TFP, one of the most potent CaM inhibitors (*23*), competes with vinblastine for CaM binding (*14*). We measured competition between TFP and VFL to locate the VFL binding site on CaM. Since controversy still remains concerning TFP binding to CaM, we measured TFP binding using ITC. We found two sets of sites: one with high affinity and four sites with lower affinity (Table 1). No ITC signal was detected during

Table 1: Thermodynamic Parameters of *Vinca* Alkaloids and STP23 Binding to Ca^{2+}−Calmodulin at 25 °C in 50 mM Hepes Buffer in the Presence of 2 mM $CaCl_2$ and 150 mM KCl, pH 7.5

ligand[a]	N	K_a (M^{-1})	ΔH (kJ/mol)	$-T\Delta S$ (kJ/mol)
VLB	0.82 ± 0.14	$(3.2 \pm 1.3) \times 10^5$	8.8 ± 2.5	-40.2
VLB^{II}	1.00	$(2.0 \pm 0.3) \times 10^4$	4.2 ± 1.2	-28.8
VLB^{amm}	0.62 ± 0.22	$(7.5 \pm 2.4) \times 10^5$	23.2 ± 4.4	-56.7
VLB^{VFL}	0.89 ± 0.14	$(2.9 \pm 1.3) \times 10^5$	8.7 ± 2.5	-40.0
VFL	0.95 ± 0.05	$(4.1 \pm 0.8) \times 10^5$	-25.1 ± 3.3	-7.0
VFL^{II}	no ITC signal			
VFL^{amm}	0.87 ± 0.05	$(7.4 \pm 0.9) \times 10^5$	-32.1 ± 3.5	-1.4
VFL^{VLB}	0.76 ± 0.05	$(1.2 \pm 1.8) \times 10^4$	-24.4 ± 3.2	-5.0
TFP	1.04 ± 0.11	$(7.6 \pm 2.1) \times 10^6$	-6.9 ± 1.2	-32.4
TFP	3.78 ± 0.12	$(5.8 \pm 1.2) \times 10^5$	-1.9 ± 0.6	-31.0
VFL^{TFP}	no ITC signal			
VLB^{TFP}	0.91 ± 0.08	$(8.0 \pm 2.1) \times 10^4$	9.1 ± 1.3	-37.1
STP23	1.00 ± 0.04	$(6.7 \pm 3.7) \times 10^5$	-23.4 ± 0.8	-9.9
STP23*	0.86 ± 0.08	$(5.0 \pm 1.4) \times 10^5$	-28.2 ± 1.1	-4.4
$STP23^{VLB}$	0.81 ± 0.12	$(5.1 \pm 2.5) \times 10^5$	-17.8 ± 0.9	-14.8
$STP23^{VFL}$	no ITC signal			

[a] Key: superscript II, thermodynamic parameters of the second binding site on Ca^{2+}−CaM calculated from the competition experiments (see details in the text); superscript amm, experiments were carried out in 10 mM ammonium bicarbonate buffer in the presence of 2 mM $CaCl_2$, pH 7.5; superscript VFL, experiments were carried out in a 3-fold excess of VFL; superscript VLB, experiments were carried out in a 3-fold excess of VLB; *, experiments were carried out without KCl; VFL^{TFP}, experiments were carried out in a 1.5-fold excess of TFP; VLB^{TFP}, experiments were carried out in a 2-fold excess of TFP.

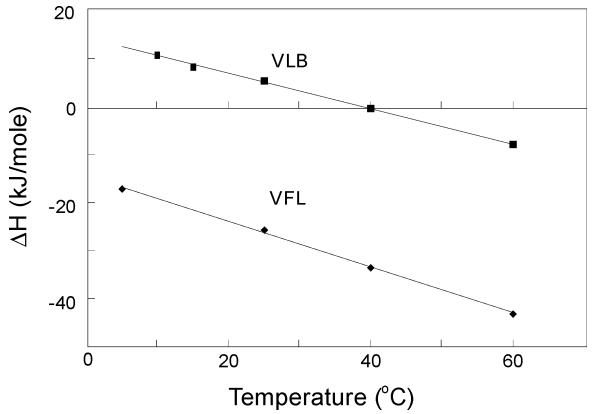

FIGURE 4: Temperature dependence of the enthalpy of VLB (top line) and VFL (bottom line) binding to Ca^{2+}−CaM in 50 mM Hepes buffer in the presence of 2 mM $CaCl_2$ and 150 mM KCl, pH 7.5. Measured ΔH values are shown as symbols, and the solid line represents the linear least-squares best fit to the data.

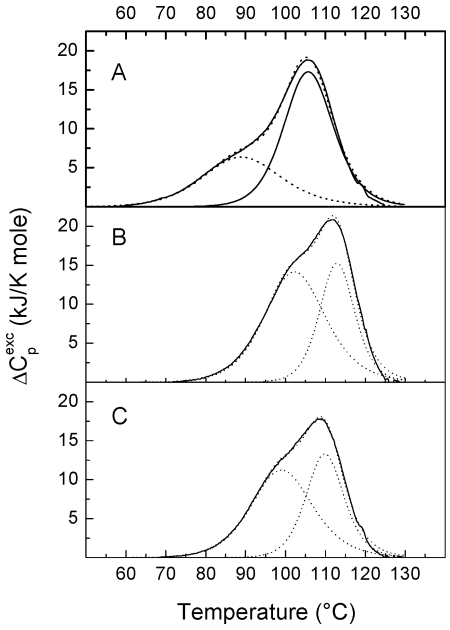

FIGURE 5: Temperature dependence of the excess heat capacity of CaM (A) and its complexes with VFL (B) and VLB (C) in 50 mM Hepes buffer in the presence of 2 mM $CaCl_2$ and 150 mM KCl, pH 7.5: solid line, experimental results; dotted lines, deconvoluted peaks and their sum.

Table 2: Thermodynamic Parameters of Ca^{2+}−Calmodulin and Ca^{2+}−Calmodulin−Ligand Complex Denaturation in 50 mM Hepes Buffer in the Presence of 2 mM $CaCl_2$ and 150 mM KCl, pH 7.5

	first transition		second transition	
sample	$T^{(1)}$ (°C)	$\Delta H_{cal}^{(1)}$ (kJ/mol)	$T^{(2)}$ (°C)	$\Delta H_{cal}^{(2)}$ (kJ/mol)
CaM	89.3	167	105.9	287
CaM−STP23	89.5	170	106.2	291
CaM−VLB	99.3	230	109.9	168 (386[a])
CaM−VFL	102.5	288	113.0	179 (423[a])

[a] Van't Hoff enthalpy values were determined by deconvolution analysis of the heat absorption curves to non-two-state transitions.

CaM titration by VFL in the presence of a 1.5-fold excess of TFP (1.5:1 TFP:CaM ratio). Nevertheless, a 2-fold excess of TFP did not change dramatically the thermodynamic parameters of VLB binding to CaM (Table 1). Neither of the *Vinca* alkaloids was able to bind to the protein in the presence of a 10-fold excess of TFP.

Thermal Denaturation of CaM−Vinca Alkaloid Complexes. The thermal denaturation of alkaloid−CaM complexes was carried out by DSC (Figure 5). The temperature dependence of the partial molar heat capacity of free Ca^{2+}−CaM considerably differs from that of its complexes with both *Vinca* alkaloids (Figure 5, Table 2). Only the first transition of the CaM−VFL and CaM−VLB denaturation is the two-state transition, while the second one is affected by irreversible processes at high temperatures. The first deconvoluted peak corresponds to the C-terminal lobe melting, and the second one is attributed to the N-terminal lobe unfolding (*20*, *24*). VFL and VLB binding to calmodulin causes a marked increase in both the thermostability of C- and N-terminal domains and the melting enthalpy (Table 2), while Ca^{2+}−CaM−STP23 complex formation does not influence the thermodynamic parameters of calmodulin denaturation (Table 2).

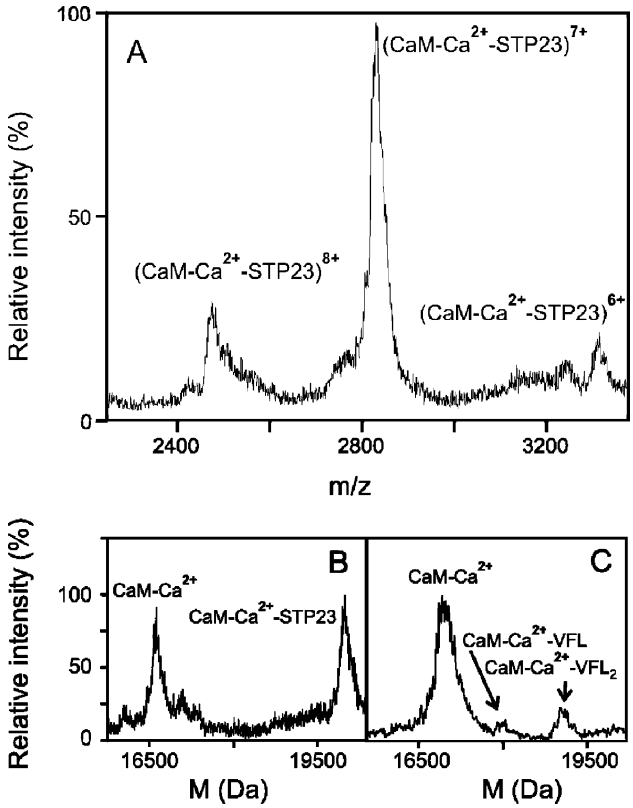

FIGURE 6: (A) ESI-MS spectrum of the Ca^{2+}−CaM−STP23 complex in 10 mM ammonium bicarbonate. The concentrations were 15 μM for CaM, 75 μM for STP23, and 200 μM for $CaCl_2$. (B) Deconvoluted spectrum of the Ca^{2+}−CaM−STP23 complex. (C) ESI-MS spectrum of STP23 binding in the presence of VFL. The concentrations were 15 μM for CaM, 75 μM for STP23, 150 μM for VFL, and 200 μM for $CaCl_2$. In the labels Ca^{2+} indicates calcifed species. The most abundant species carried four calcium ions.

Vinflunine Inhibits STP23 Peptide Binding to CaM. STP23 binding to CaM was measured by ESI-MS under nondenaturing conditions. In the absence of calcium there is no experimental evidence of the CaM−STP23−*Vinca* alkaloid complex (not shown). In 200 μM $CaCl_2$, in the presence of a 5-fold excess of peptide (75 μM) we detected peaks corresponding to the charge states of the Ca^{2+}−CaM−STP23 complex (Figure 6A). Its molecular mass is 19700 Da (Figure 6C). In the presence of a 2-fold excess of VFL these peaks were no longer detectable (Figure 6C), but the CaM−VFL complex was present. In the presence of the same excess of VLB, peaks corresponding to the Ca^{2+}−CaM−STP23 complex were still present. An increase in VLB concentration in the solution (more than 15-fold excess compared to the peptide) abolished the peaks corresponding to the Ca^{2+}−CaM−peptide complex.

As demonstrated by ITC, the STP23 peptide binds to CaM with a constant of 6.7×10^5 M^{-1} (Figure 7, Table 1), which agrees with the results of Bouvier et al. obtained by fluorescence (*10*) and is in the range of the reported values for the CaM−F−STOP binding affinities (*9*). STP23 binding to CaM is an enthalpically and entropically favorable process (Table 1). Contrary to the previously published data (*10*), we observed peptide binding both at low salt concentration and in physiologically relevant conditions (150 mM KCl) without changes in the binding affinity (Table 1). As shown in Figure 7C where traces correspond only to the dilution

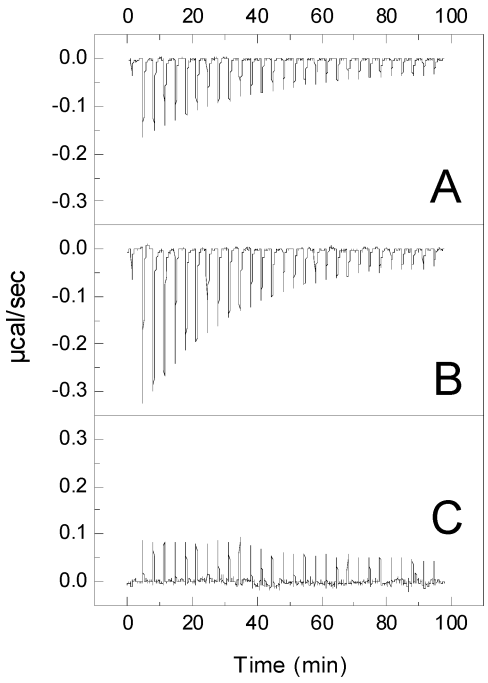

FIGURE 7: ITC curves of the CaM−STP23 interaction at 25 °C in 50 mM Hepes buffer in the presence of 2 mM $CaCl_2$, pH 7.5: (A) without *Vinca* alkaloid, (B) with a 3-fold excess of VLB, (C) with a 3-fold excess of VFL.

effect, ITC data show that a 3-fold excess of VFL totally inhibits STP23 interaction with CaM, whereas in the presence of a 3-fold excess of VLB binding of STP23 to Ca^{2+}−CaM is not modified (Figure 7). However, a larger excess of VLB (15-fold) inhibits this interaction (Table 1).

DISCUSSION

Vinflunine, a novel microtubule inhibitor in phase III clinical trials, exceeds other *Vinca* alkaloids in their effects on a number of tumors such as renal and small-cell lung cancer (*25*), despite an overall affinity for tubulin several-fold lower than that of vinblastine or vincristine (*18*). Data from Jordan and co-workers showed that intracellular levels of VFL were more than 10-fold higher than those of VLB in HeLa cells. Interestingly, almost all microtubules treated with VFL remained intact, suggesting that VFL was not able to bind to tubulin and most of the drug appeared in different cell compartments (*13*). Therefore, VFL may be gradually released, thereby prolonging its therapeutic activity and providing low toxicity. On the basis of the work of Vertessy et al. on VLB binding to CaM (*14*), we propose that CaM could be a potential target for VFL. Our data show that VFL binds to calmodulin on a different site than VLB. Moreover, as shown by ΔC_p values and DSC measurements, it induces different conformational changes. We can therefore estimate that the difference between the two *Vinca* alkaloids in the binding parameters measured by ITC relies on the binding per se of the molecule. Structurally, VFL differs from VLB by the selective introduction of the two fluorine atoms on the cleavamine moiety by superacid chemistry (Figure 1), a part of the molecule that was previously inaccessible by classical chemistry (*16*). The two drugs demonstrate opposite thermodynamic binding profiles to CaM: VFL binding is more polar in nature, while the VLB association is driven by hydrophobic forces (Table 1). It is reasonable to connect this chemical modification to the observed differences in binding behavior to CaM, making modification of the cleavamine part critical for the *Vinca* alkaloid−CaM interaction. With regard to VFL, the presence of the fluorine atoms induces positioning of the molecule favoring a specific bonding network. The exothermic character of the binding is consistent with the existence of additional hydrogen bonds.

There is an apparent controversy between ITC and mass spectrometry results. While mass spectrometry shows up to three molecules of *Vinca* alkaloids bound to CaM with a predominant 2:1 complex, ITC measurements were only able to confirm the binding of two *Vinca* alkaloid molecules on two different sites: one via direct binding and another via ITC competition experiments. The VFL binding site has low affinity for VLB and vice versa. The small enthalpy of binding for the second binding event, i.e., the lowest affinity site for each drug (Table 1), explains the absence of detection by direct ITC measurements. The third Vinca alkaloid site detected by mass spectrometry is probably too weak to be detected by ITC.

DSC measurements show the increase in thermostability of both C- and N-terminal domains of CaM upon VLB or VFL binding, demonstrating that binding of the two *Vinca* alkaloids affects both CaM domains. It is also interesting to note that the influence of VFL on the thermostability of the N-terminal domain of CaM exceeds the influence of VLB. This is in good agreement with ΔC_p values which indicate stronger conformational changes of CaM upon VFL binding. VFL binds to CaM with a K_d of 2.4 μM. This binding constant is compatible with biological effects if we consider that microtubule inhibitors accumulate in cells (*26*). Dhamodharan et al. demonstrated that the intracellular concentration of VLB can reach 250 times the extracellular concentration (*27*).

NMR has demonstrated that STP23 peptide binding to Ca^{2+}−CaM is not typical and mostly involves its C-terminal domain, with CaM remaining in an extended conformation (*10*). Our DSC data confirm that peptide binding does not produce major conformational changes in the three-dimensional structure since the thermal stability of both calmodulin domains is not modified (Table 2). The STP23 binding site on CaM is closely related to the TFP1 binding site described by Vandonselaar et al. (*23*). Indeed, Bouvier et al. demonstrated that 9 residues out of 13 having contacts with TFP in the Ca^{2+}−CaM−TFP complex are also involved in STP23 binding (*10*). Can VFL bind to the TFP1 site? Our ITC experiments have shown that five TFP binding sites exist on our calmodulin in agreement with the previously published data (*28*). One site has high affinity for TFP, and four sites have 10-fold lower affinity (Table 1). X-ray crystallographic structures of Ca^{2+}−CaM−TFP complexes were obtained with 1:1, 1:2, and 1:4 CaM:TFP ratios. The common binding site of these three structures is located in the C terminus of CaM and labeled TFP1. The binding of one TFP molecule is sufficient to induce a major conformational change in CaM. The complexes of Ca^{2+}−CaM with one, two, or four TFP bound are very similar and adopt a compact globular structure not compatible with peptide binding (*29*). A weak excess of TFP abolishes VFL binding; i.e., TFP may saturate the high-affinity site TFP1, which is also the binding site for VFL.

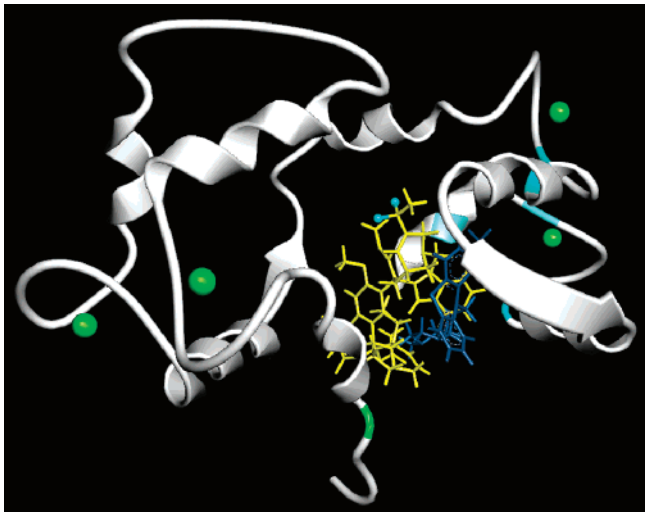

FIGURE 8: Proposed binding mode of vinflunine to Ca^{2+}−CaM obtained with molecular docking using ArgusLab (Planaria Software LLC, Seattle, WA). The protein originates from the X-ray structure of its complex with trifluoperazine (encoded as 1A29 in PDB). Trifluoperazine is in dark blue [TFP1, as numerically labeled by Vandonselaar et al. (*23*)], VFL is in yellow with fluorine atoms in light blue, and CaM is shown in gray ribbon representation. The four calcium atoms are in green. The orientation of the arrows representing β strands indicates the direction of the polypeptide chain (N to C terminus).

On the basis of the information presented above, we propose in Figure 8 a model for the binding of VFL to the most suitable TFP binding site of CaM. To obtain our model, we tried to dock VFL in the two TFP binding sites of the 1A29 PDB structure of CaM. The best docking was obtained on the TFP1 binding site. In the proposed model, VFL forms a hydrogen bond with E8 of the N-terminal domain of CaM, which could explain the stabilization of the domain seen by DSC and also the exothermic character of the binding.

TFP inhibits cell migration and differentiation and impairs in vitro endothelial cell differentiation into tubelike structures (*30*), showing that CaM is involved in angiogenesis. We have shown that VFL at antiangiogenic concentrations has the same inhibitory effect on cell migration (*31*). We can hypothesize that the antiangiogenic effect of VFL may involve CaM.

Perhaps more critical to microtubule dynamics in mitotic cells is that VFL is a better competitor for CaM interaction with STOP than VLB. The consequence of the partial modification of the cleavamine molecule is that now a high-affinity binding site for VFL is closely related to the first TFP binding site, and therefore, steric hindrance could occur between VFL and STP23. Since the binding of VLB is still possible when TFP binds to CaM (Table 1), showing competition between the two molecules, we propose that the VLB high-affinity binding site is located closer to another TFP binding pocket, noncritical for Ca^{2+}−CaM−STP23 interaction. Hence, VLB perturbs CaM−STOP interaction at a higher concentration via its low-affinity site, which is also the VFL high-affinity site.

The demonstrated VFL effect on CaM−STOP complex formation suggests that the drug influences the microtubule dynamics not only via direct contacts with tubulin but also via other proteins involved in the network of microtubule stability regulation. As is widely accepted, the microtubule-associated protein STOP plays a key role in mitosis (*32*). In fact, in proliferative cells, such as cancer cells, STOP is associated with the microtubule spindle (*33*). Its inactivation by Ca^{2+}−CaM enhances the microtubule dynamics and thus allows mitosis completion (*8*, *34*). As with other *Vinca* alkaloids, VFL suppresses microtubule dynamics both in vitro (*35*) and in cancer cells (*36*), inducing mitotic block and apoptosis (*36*, *37*). VFL inhibition of the STOP−CaM interaction may maintain STOP on the spindle microtubules and thus intensify the microtubule dynamics suppression and disrupt the mitotic progression. This additional activity of VFL on CaM combined with its binding to tubulin may potentiate its antitumor effects and indicate the potential clinical relevance of targeting CaM−STOP interaction.

ACKNOWLEDGMENT

We thank Dr. Pascal Verdier-Pinard for critical reading of the manuscript.

SUPPORTING INFORMATION AVAILABLE

Scheme of VFL and VBL binding to CaM. This material is available free of charge via the Internet at http://pubs.acs.org.

REFERENCES

1. Margolis, R. L., Rauch, C. T., and Job, D. (1986) Purification and assay of a 145-kDa protein (STOP 145) with microtubule-stabilizing and motility behavior, *Proc. Natl. Acad. Sci. U.S.A. 83*, 639−643.
2. Pabion, M., Job, D., and Margolis, R. L. (1984) Sliding of STOP proteins on microtubules, *Biochemistry 23*, 6642−6648.
3. Andrieux, A., Salin, P. A., Vernet, M., Kujala, P., Baratier, J., Gory-Fauré, S., Bosc, C., Pointu, H., Proietto, D., Schweitzer, A., Denarier, E., Klumperman, J., and Job, D. (2002) The suppression of brain cold-stable microtubules in mice induces synoptic defects associated with neuroleptic-sensitive behavioral disorders, *Genes Dev. 16*, 2350−2364.
4. Denarier, E., Fourest-Lieuvin, A., Bosc, C., Pirollet, F., Chapel, A., Margolis, R. L., and Job, D. (1998) Nonneuronal isoforms of STOP protein are responsible for microtubule cold stability in mammalian fibroblasts, *Proc. Natl. Acad. Sci. U.S.A. 95*, 6055−6060.
5. Pirollet, F., Derancourt, J., Haiech, J., Job, D., and Margolis, R. L. (1992) Ca^{2+}-calmodulin regulated effectors of microtubule stability in bovine brain, *Biochemistry 31*, 8849−8855.
6. Pirollet, F., Margolis, R. L., and Job, D. (1992) Ca^{2+}-calmodulin regulated effectors of microtubule stability in neuronal tissues, *Biochim. Biophys. Acta 1160*, 113−119.
7. Erent, M., Pagakis, S., Browne, J. P., and Bayley, P. M. (1999) Association of calmodulin with cytoskeletal structures at different stages of HeLa cell division, visualized by a calmodulin-EGFP fusion protein, *Mol. Cell Biol. Res. Commun. 1*, 209−215.
8. Li, C. J., Heim, R., Lu, P., Pu, Y., Tsien, R. Y., and Chang, D. C. (1999) Dynamic redistribution of calmodulin in HeLa cells during cell division as revealed by a GFP-calmodulin fusion protein technique, *J. Cell Sci. 112*, 1567−1577.
9. Bosc, C., Frank, R., Denarier, E., Ronjat, M., Schweitzer, A., Wehland, J., and Job, D. (2001) Identification of novel bifunctional calmodulin-binding and microtubule-stabilizing motifs in STOP proteins, *J. Biol. Chem. 276*, 30904−30913.
10. Bouvier, D., Vanhaverbeke, C., Simorre, J., Arlaud, G. J., Bally, I., Forge, V., Margolis, R. L., Gans, P., and Kleman, J. (2003) Unusual Ca^{2+}-calmodulin binding interactions of the microtubule-associated protein F-STOP, *Biochemistry 42*, 11484−11493.
11. Jean-Decoster, C., Brichese, L., Barret, J. M., Tollon, Y., Kruczynski, A., Hill, B. T., and Wright, M. (1999) Vinflunine, a new *Vinca* alkaloid: cytotoxicity, cellular accumulation and action on the interphasic and mitotic microtubule cytoskeleton ofPtK2 cells, *Anticancer Drugs 10*, 537−543.
12. Kruczynski, A., Colpaert, F., Tarayre, J. P., Mouillard, P., Fahy, J., and Hill, B. T. (1998) Preclinical *in vivo* antitumor activity of

vinflunine, a novel fluorinated *Vinca* alkaloid, *Cancer Chemother. Pharmacol. 41*, 437−447.
13. Ngan, V. K., Bellman, K., Hill, B. T., Wilson, L., and Jordan, M. A. (2001) Mechanism of mitotic block and inhibition of cell proliferation by the semisynthetic *Vinca* alkaloids vinorelbine and its newer derivative vinflunine, *Mol. Pharmacol. 60*, 225−232.
14. Vertessy, B. G., Harmat, V., Böcskei, Z., Náray-Szabó, G., Orosz, F., and Ovádi, J. (1998) Simultaneous binding of drugs with different chemical structures to Ca^{2+}-calmodulin: crystallographic and spectroscopic studies, *Biochemistry 37*, 15300−15310.
15. Moisoi, N., Erent, M., Whyte, S., Martin, S., and Bayley, P. M. (2002) Calmodulin-containing substructures of the centrosomal matrix released by microtubule perturbation, *J. Cell Sci. 115*, 2367−2379.
16. Bennouna, J., Campone, M., Delord, J. P., and Pinel, M. (2005) Vinflunine: a novel antitubulin agent in solid malignecies, *Expert Opin. Invest. Drugs 14*, 1259−1267.
17. Kruczynski, A., and Hill, B. T. (2001) Vinflunine, the latest *Vinca* alkaloid in clinical development. A review of itspreclinical anticancer properties, *Crit. Rev. Oncol. Hematol. 40*, 159−173.
18. Lobert, S., Ingram, J. W., Hill, B. T., and Correia, J. J. (1998) A comparison of thermodynamic parameters for vinorelbine- and vinflunine-induced tubulin self-association by sedimentation velocity, *Mol. Pharmacol. 53*, 908−915.
19. Gilli, R., Lafitte, D., Lopez, C., Kilhoffer, M., Makarov, A. A., Briand, C., and Haiech, J. (1998) Thermodynamic analysis of calcium and magnesium binding to calmodulin, *Biochemistry 37*, 5450−5456.
20. Protasevich, I. I., Ranjbar, B., Lobachov, V. M., Makarov, A. A., Gilli, R., Briand, C., Lafitte, D., and Haiech, J. (1997) Conformation and thermal denaturation of apocalmodulin: role of electrostatic mutations, *Biochemistry 36*, 2017−2024.
21. Sobott, F., McCammon, M. G., Hernández, H., and Robinson, C. V. (2005) The flight of macromolecular complexes in a mass spectrometer, *Philos. Trans.: Phys. Eng. Sci. 363*, 379−391.
22. Jelesarov, I., and Bosshard, H. R. (1999) Isothermal titration calorimetry and differential scanning calorimetry as complementary tools to investigate the energetics of biomolecular recognition, *J. Mol. Recognit. 12*, 3−18.
23. Vandonselaar, M., Hickie, R. A., Quail, J. W., and Delbaere, L. T. (1994) Trifluoperazine-induced conformational change in Ca^{2+}-calmodulin, *Nat. Struct. Biol. 1*, 795−801.
24. Tsalkova, T. N., and Privalov, P. L. (1985) Thermodynamic study of domain organization in troponin C and calmodulin, *J. Mol. Biol. 181*, 533−544.
25. Bennouna, J., Fumoleau, P., Armand, J., Raymond, E., Campone, M., Delgado, F., Puozzo, C., and Marty, M. (2003) Phase I and pharmacokinetic study of the new vinca alkaloid vinflunine administered as a 10-min infusion every 3 weeks in patients with advanced solid tumours, *Ann. Oncol. 14*, 630−637.
26. Andre, N., Braguer, D., Brasseur, G., Goncalves, A., Lemesle-Meunier, D., Guise, S., Jordan, M. A., and Briand, C. (2000) Paclitaxel induces release of cytochrome c from mitochondria isolated from human neuroblastoma cells, *Cancer Res. 60*, 5349−5353.
27. Dhamodharan, R., Jordan, M. A., Thrower, D., Wilson, L., and Wadsworth, P. (1995) Vinblastine suppresses dynamics of individual microtubules in living interphase cells, *Mol. Biol. Cell 6*, 1215−1229.
28. Massom, L. R., Lukas, T. J., Persechini, A., Kretsinger, R. H., Watterson, D. M., and Jarrett, H. W. (1991) Trifluoperazine binding to mutant calmodulins, *Biochemistry 30*, 663−667.
29. Matsushima, N., Hayashi, N., Jinbo, Y., and Izumi, Y. (2000) Ca^{2+}-bound calmodulin forms a compact globular structure on binding four trifluoperazine molecules in solution, *Biochem. J. 347*, 211−215.
30. Shen, W. G., Peng, W. X., Dai, G., Xu, J. F., Zhang, Y., and Li, C. J. (2007) Calmodulin is essential for angiogenesis in response to hypoxic stress in endothelial cells, *Cell Biol. Int. 31*, 126−134.
31. Pourroy, B., Honore, S., Pasquier, E., Bourgarel-Rey, V., Kruczynski, A., Briand, C., and Braguer, D. (2006) Antiangiogenic concentrations of vinflunine increase the interphase microtubule dynamics and decrease the motility of endothelial cells, *Cancer Res. 66*, 3256−3263.
32. Bosc, C., Oenarier, E., Andrieux, A., and Job, D. (1999) Stop proteins, *Cell Struct. Funct. 24*, 393−399.
33. Margolis, R. L., Rauch, C. T., Pirollet, F., and Job, D. (1990) Specific association of STOP protein with microtubules in vitro and with stable microtubules in mitotic spindles of cultured cells, *EMBO J. 9*, 4095−4102.
34. Erent, M., Pagakis, S., Browne, J. P., and Bayley, P. (1999) Association of calmodulin with cytoskeletal structures at different stages of HeLa cell division, visualized by a calmodulin-EGFP fusion protein, *Mol. Cell Biol. Res. Commun. 1*, 209−215.
35. Ngan, V. K., Bellman, K., Panda, D., Hill, B. T., Jordan, M. A., and Wilson, L. (2000) Novel actions of the antitumour drugs vinflunine and vinorelbine on microtubules, *Cancer Res. 60*, 5045−5051.
36. Pourroy, B., Carre, M., Honore, S., Bourgarel-Rey, V., Kruczynski, A., Briand, C., and Braguer, D. (2004) Low concentrations of vinflunine induce apoptosis in human SK-N-SH neuroblastoma cells through a postmitotic G1 arrest and a mitochondrial pathway, *Mol. Pharmacol. 66*, 580−591.
37. Kruczynski, A., and Hill, B. T. (2001) Vinflunine, the latest *Vinca* alkaloid in clinical development. A review of its preclinical anticancer properties, *Crit. Rev. Oncol. Hematol. 40*, 159−173.

BI701803S